

# Strong squeezing via phonon mediated spontaneous generation of photon pairs

Kenan Qu and G. S. Agarwal

*Department of Physics, Oklahoma State University, Stillwater, Oklahoma, 74078, USA*

(Dated: December 3, 2024)

We propose a scheme generating robust squeezed light by using double cavity optomechanical system driven by blue detuned laser in one cavity and by red detuned laser in the other. This double cavity system is shown to mimic effectively an interaction that is similar to the one for the downconverter, which is known to be a source of strong squeezing for the light fields. There are however distinctions as the phonons, which lead to such an interaction, can contribute to the quantum noise. We show that the squeezing of the output fields of the order of 10dB can be achieved even at mirror temperature of the order 10mK.

PACS numbers: 42.50.Wk, 42.50.Dv, 07.10.Cm

## I. INTRODUCTION

Realization of the quantum regime [1–17] of physical systems has been of great interest. One important signature of the quantum regime is the squeezing which has been studied rather extensively for radiation fields [18–20], collection of two level atoms and spins [21, 22], optical phonons [23], and Bose condensates [24–27]. The squeezing is of fundamental importance in precision measurements [28–30] and thus quantum metrology drives the demand not only for higher levels of squeezing but also availability of squeezing in a variety of systems. There are several studies demonstrating squeezing in optomechanical systems [7, 31–37].

The recently reported ponderomotive squeezing of light [3, 34–36] utilizes a driving field on resonance to the cavity frequency and generates squeezed light near the side-band of the driving field. In optomechanical ponderomotive squeezing, the quantum noise of light is reduced by using radiation pressure to push on the mechanical vibrating membrane that, in turn, feeds back on the light's phase. The degree of noise reduction depends heavily on the optomechanical coupling strength which is in favor of a higher cavity finesse. However, high cavity finesse limits the squeezed output intensity since it is off-resonant to the cavity. We note that the nondegenerate downconverter is now the standard source for producing squeezed light though one needs much larger nonlinearity to produce large amounts of squeezing. The latter is a challenge. In the present paper, we discuss an optomechanical system where we produce photon pairs in a way similar to downconverter. However, for the optomechanical system, phonons mediate the interactions and provide the source of active nonlinearity. We show generation of very large squeezing even at a temperature like 10mK. The large squeezing is a consequence of active phonon nonlinearities which become large due to the resonant nature of the underlying processes.

The downconverter is the work horse of quantum optical experiments on entangled and squeezed light [18–20]. In a downconverter, three light field modes  $a$ ,  $b$  and  $c$  get coupled in a nonlinear medium where the second order nonlinearity is nonzero. This coupling is described by

the Hamiltonian  $\chi a^\dagger b c + \chi a b^\dagger c^\dagger$  which, under the condition of a strong undepleted pump field  $a$ , reduces to  $\xi b c + \xi^* b^\dagger c^\dagger$ . The photon pairs  $b$  and  $c$  are spontaneously produced from the pump. These are the entangled pairs. An appropriate linear combinations  $(b + c e^{i\theta})/\sqrt{2}$  of the modes  $b$  and  $c$  can produce quadrature squeezing. Note that the susceptibility  $\chi$  for the downconverter has no resonances in the frequency range of interest. Any system where the effective interaction that can be reduced to the form  $\xi b c + \xi^* b^\dagger c^\dagger$  becomes a good candidate for squeezing. The third order nonlinearities in optical fibers can give rise to such an interaction leading to a large number of studies on squeezing. The optical phonons in crystals also yield such an interaction and squeezing of optical phonons has been demonstrated. For the cavity optomechanics, one has the well-known parametric process: A blue detuned pump with frequency  $\omega_l$  can in fact produce spontaneously a cavity photon of frequency  $\omega_c$  and a phonon of frequency  $\omega_m$ . In the undepleted pump approximation, this process would be described by an effective Hamiltonian  $\xi b c + \xi^* b^\dagger c^\dagger$  where  $b$  stands for the cavity photon and  $c$  stands for the phonon. Though this Hamiltonian has the form of a downconverter, it cannot produce squeezing of the light field since  $\omega_m$  is many orders less than  $\omega_c$ . The cavity optomechanics has another parametric process where a red detuned pump and a probe can produce a coherent phonon. In the undepleted pump approximation, this is described by  $\xi b^\dagger c + \xi^* b c^\dagger$ . This interaction also implies that a phonon in combination with a red detuned pump will produce a cavity photon. Thus a cavity photon can be produced using either the blue detuned pump or by using a red detuned pump and a phonon. In what follows, we use both these mechanisms to produce a pair of photons in a double cavity optomechanical system. Thus we produce a photon pair by using phonons. It should be kept in mind that although we produce a photon pair, the mediating mechanism is an active mechanism which puts a limit on the amount of achievable squeezing. This is in contrast to the situation with a downconverter where the crystal participates in a passive manner in the sense that it does not contribute to quantum noise.

## II. MODEL AND FLUCTUATING QUANTUM FIELDS

We consider a double cavity optomechanical system model [38], in which a mechanical resonator coated with perfect reflecting films on both sides are coupled to two identical optical cavities. In optomechanics, we denote

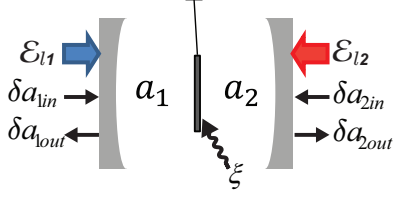


FIG. 1: Schematic of the proposed double cavity optomechanics where cavity 1 (2) fed by blue (red) detuned driving lasers and vacuum inputs are coupled to the same mechanical resonator mediated in thermal bath.  $\mathcal{E}_i$ ,  $a_i$ ,  $\delta a_{i\text{in}}$  and  $\delta a_{i\text{out}}$  denote the classical driving field, in-cavity optical field, input quantum vacuum noise and output quantum fluctuation for cavity  $i$ , respectively, and  $\xi$  denotes the mechanical noise.

the optical modes using the annihilation operators  $a_i$  for the cavity  $i$  and the mechanical mode of the resonator using the normalized displacement operator  $Q = \sqrt{m\omega_m/\hbar}q$  and momentum operator  $P = 1/\sqrt{m\hbar\omega_m}p$  where  $q$ ,  $p$ ,  $m$  and  $\omega_m$  are the displacement, momentum, mass and the oscillation frequency of the mirror, respectively. The interaction between the optical and mechanical modes arises from the radiation pressure of light  $-(\hbar\omega_{ci}/L_i)qa_i^\dagger a_i = -\hbar g Q a_i^\dagger a_i$ , where  $\omega_{ci}$  and  $L_i$  are the resonance frequency and length of the empty cavity  $i$ . We denote the coupling rate by  $g_i = \frac{\omega_{ci}}{L_i} \sqrt{\frac{\hbar}{m\omega_m}}$ . In order to enhance the optomechanical coupling, a driving laser with an amplitude  $\mathcal{E}_i$  and frequency  $\omega_{li}$  is applied to each cavity. We treat the driving lasers classically since they are strong. Then the Hamiltonian for the system can be written as

$$H = \sum_{i=1,2} [\hbar\omega_{ci}a_i^\dagger a_i + i\hbar\mathcal{E}_i e^{-i\omega_{li}t}(a_i^\dagger - a_i)] + \frac{1}{2}\hbar\omega_m(Q^2 + P^2) - \hbar(g_1a_1^\dagger a_1 - g_2a_2^\dagger a_2)Q. \quad (1)$$

It is convenient to rewrite the Hamiltonian into a new picture using transformation  $\exp[-i\sum(\omega_{li}a_i^\dagger a_i t)]$ , then

$$H = \sum_{i=1,2} [\hbar(\omega_{ci} - \omega_{li})b_i^\dagger b_i + i\hbar\mathcal{E}_i(b_i^\dagger - b_i)] + \frac{1}{2}\hbar\omega_m(Q^2 + P^2) - \hbar(g_1b_1^\dagger b_1 - g_2b_2^\dagger b_2)Q, \quad (2)$$

with  $b_i$ 's defined by  $a_i = b_i e^{-i\omega_{li}t}$ . The driving laser amplitude is related to its power  $\mathcal{P}_i$  by  $\mathcal{E}_i = \sqrt{2\kappa\mathcal{P}_i/(\hbar\omega_{li})}$  and  $2\kappa_i$  is the decay rate of the cavity  $i$ . The quantum Langevin equations governing the system can be obtained

by using the Heisenberg equation and adding the corresponding decay terms and the input noise terms,

$$\begin{aligned} \dot{Q} &= \omega_m P, \\ \dot{P} &= g(b_1^\dagger b_1 - b_2^\dagger b_2) - \omega_m Q - \gamma_m P + \xi, \\ \dot{b}_1 &= -i(\omega_{c1} - \omega_{l1} - gQ)b_1 - \kappa_1 b_1 + \mathcal{E}_{l1} + \sqrt{2\kappa_1}b_{1\text{in}}, \\ \dot{b}_2 &= -i(\omega_{c2} - \omega_{l2} + gQ)b_2 - \kappa_2 b_2 + \mathcal{E}_{l2} + \sqrt{2\kappa_2}b_{2\text{in}}, \end{aligned} \quad (3)$$

where  $b_{1\text{in}}$  and  $b_{2\text{in}}$  are the optical input vacuum noise with correlation relation

$$\langle b_{i\text{in}}(t)b_{j\text{in}}^\dagger(t') \rangle = \delta_{ij}\delta(t-t') \quad (4)$$

and  $\xi$  stems from the thermal noise of the mechanical resonator at finite temperature, which obeys

$$\langle \xi(t)\xi(t') \rangle = \frac{\gamma_m}{2\pi\omega_m} \int \omega e^{-i\omega(t-t')} \left[ 1 + \coth\left(\frac{\hbar\omega}{2K_B T}\right) \right] d\omega,$$

where  $K_B$  is the Boltzmann constant and  $T$  is the temperature. We follow the typical procedure and solve Eq. (3) perturbatively by separating the classical mean value and the fluctuation of each operator,

$$Q = Q_s + \delta Q, \quad P = P_s + \delta P, \quad b_i = b_{is} + \delta b_i, \quad (5)$$

and  $i = 1, 2$ . In this way, we can solve for the classical mean values of the optical fields as  $b_{is} = \frac{\mathcal{E}_i}{\kappa_i + i\Delta_i}$  and  $Q_s = (|b_{1s}|^2 g_1 - |b_{2s}|^2 g_2)/\omega_m$  where  $\Delta_i = \omega_{ci} - \omega_{li} \mp g_i Q_s$  are the mean detuning of the cavities and  $-$  is for  $i = 1$  and  $+$  for  $i = 2$ . Then the linearized quantum Langevin equations are given by

$$\begin{aligned} \delta\dot{Q} &= \omega_m \delta P, \\ \delta\dot{P} &= g_1(b_{1s}^* \delta b_1 + b_{1s} \delta b_1^\dagger) - g_2(b_{2s}^* \delta b_2 + b_{2s} \delta b_2^\dagger) \\ &\quad - \omega_m \delta Q - \gamma_m \delta P + \xi, \\ \delta\dot{b}_1 &= -(\kappa_1 + i\Delta_1)\delta b_1 + ig_1 b_{1s} \delta Q + \sqrt{2\kappa_1}b_{1\text{in}}, \\ \delta\dot{b}_2 &= -(\kappa_2 + i\Delta_2)\delta b_2 - ig_2 b_{2s} \delta Q + \sqrt{2\kappa_2}b_{2\text{in}}, \end{aligned} \quad (6)$$

It is convenient to work with the new optical and mechanical annihilation operators defined as

$$\begin{aligned} \tilde{b}_1 &= \delta b_1 e^{-i\omega_m t}, & c e^{-i\omega_m t} &= (\delta Q + \delta P)/\sqrt{2}, \\ \tilde{b}_2 &= \delta b_2 e^{i\omega_m t}, & c^\dagger e^{i\omega_m t} &= (\delta Q - \delta P)/(\sqrt{2}i). \end{aligned} \quad (7)$$

These operators obey the equations

$$\begin{aligned} \dot{c} &= -\frac{\gamma_m}{2}(c - c^\dagger e^{2i\omega_m t}) + f(t) \\ &\quad + i\frac{g_1}{\sqrt{2}}(b_{1s}^* \tilde{b}_1 e^{2i\omega_m t} + b_{1s} \tilde{b}_1^\dagger) \\ &\quad - i\frac{g_2}{\sqrt{2}}(b_{2s}^* \tilde{b}_2 + b_{2s} \tilde{b}_2^\dagger e^{2i\omega_m t}), \\ \dot{\tilde{b}}_1 &= -(\kappa_1 + i\Delta_1 + i\omega_m)\delta b_1 + \sqrt{2\kappa_1}\tilde{b}_{1\text{in}} \\ &\quad + i\frac{g_1}{\sqrt{2}}b_{1s}(c e^{-2i\omega_m t} + c^\dagger), \\ \dot{\tilde{b}}_2 &= -(\kappa_2 + i\Delta_2 - i\omega_m)\delta b_2 + \sqrt{2\kappa_2}\tilde{b}_{2\text{in}} \\ &\quad - i\frac{g_2}{\sqrt{2}}b_{2s}(c + c^\dagger e^{2i\omega_m t}). \end{aligned} \quad (8)$$

The rapidly rotating terms in (8) correspond to nonresonant four-wave mixing (FWM) processes, for example in cavity 2 a red pump  $\omega_c - \omega_m$  and a probe  $\omega_c$  can produce a photon of frequency  $\omega_c - 2\omega_m$  and a photon of frequency  $\omega_c$ . The generation at  $\omega_c$  is a resonant process whereas the generation at  $\omega_c - 2\omega_m$  is a nonresonant process. We drop all the nonresonant processes. Thus by dropping rapidly rotating terms at frequencies  $2\omega_m$ , we obtain

$$\begin{aligned}\dot{c} &= -\frac{\gamma_m}{2}c + f(t) + iG_1\tilde{b}_1^\dagger - iG_2^*\tilde{b}_2, \\ \dot{\tilde{b}}_1^\dagger &= -(\kappa_1 - ix_1)\tilde{b}_1^\dagger - iG_1^*c + \sqrt{2\kappa_1}\tilde{b}_{1\text{in}}^\dagger, \\ \dot{\tilde{b}}_2 &= -(\kappa_2 + ix_2)\tilde{b}_2 - iG_2c + \sqrt{2\kappa_2}\tilde{b}_{2\text{in}},\end{aligned}\quad (9)$$

where  $x_1 = \Delta_1 + \omega_m$ ,  $x_2 = \Delta_2 - \omega_m$  and  $G_i = b_{is}g_i/\sqrt{2}$  for  $i = 1, 2$ . Notice that  $G_i$  is a pure imaginary number by definition of  $b_{is}$  under resolved side-band regime,  $\Delta \gg \kappa_i$ . Since the coupling laser in cavity 1(2) is blue(red) detuned by an amount  $\omega_m$ ,  $x_1 \sim x_2 \sim 0$ .  $f(t)$  has the correlation relation

$$\begin{aligned}\langle f(t)f^\dagger(t') \rangle &= \gamma_m(\bar{n}_{\text{th}} + 1)\delta(t - t'), \\ \langle f^\dagger(t)f(t') \rangle &= \gamma_m\bar{n}_{\text{th}}\delta(t - t'),\end{aligned}\quad (10)$$

where  $\bar{n}_{\text{th}}(\omega) = [\exp(\hbar\omega/K_B T) - 1]^{-1}$  is the mean phonon number at temperature  $T$ . In order to solve these equations, we transform them into the frequency domain using  $A(t) = \frac{1}{2\pi} \int_{-\infty}^{+\infty} A(\omega)e^{-i\omega t}d\omega$ , and  $A^\dagger(t) = \frac{1}{2\pi} \int_{-\infty}^{+\infty} A^\dagger(-\omega)e^{-i\omega t}d\omega$ , so that  $A^\dagger(-\omega) = [A(-\omega)]^\dagger$ . Then the correlation relation is  $\langle \tilde{b}_i(\omega)\tilde{b}_j^\dagger(-\omega') \rangle = 2\pi\delta_{ij}\delta(\omega + \omega')$ . Using the input-output relations  $\tilde{b}_{i\text{out}} = \sqrt{2\kappa_i}\tilde{b}_i - \tilde{b}_{i\text{in}}$ , the output optical fields can be calculated as

$$\begin{aligned}\tilde{b}_{1\text{out}}(\omega) &= E_1(\omega)\tilde{b}_{1\text{in}}(\omega) + F_1(\omega)\tilde{b}_{2\text{in}}^\dagger(-\omega) \\ &\quad + V_1(\omega)f^\dagger(-\omega),\end{aligned}\quad (11)$$

$$\begin{aligned}\tilde{b}_{2\text{out}}(\omega) &= E_2(\omega)\tilde{b}_{2\text{in}}(\omega) + F_2(\omega)\tilde{b}_{1\text{in}}^\dagger(-\omega) \\ &\quad + V_2(\omega)f(\omega),\end{aligned}\quad (12)$$

where

$$\begin{aligned}E_1(\omega) &= \frac{2\kappa_1}{D^*(-\omega)} \frac{|G_1|^2}{(\kappa_1 + ix_1 + i\omega)^2} + \frac{2\kappa_1}{\kappa_1 + ix_1 + i\omega} - 1, \\ F_1(\omega) &= -\frac{\sqrt{2\kappa_1 2\kappa_2} G_1^* G_2}{D^*(-\omega)(\kappa_1 + ix_1 + i\omega)(\kappa_2 - ix_2 - i\omega)}, \\ E_2(\omega) &= -\frac{2\kappa_2}{D(\omega)} \frac{|G_2|^2}{(\kappa_2 + ix_2 - i\omega)^2} + \frac{2\kappa_2}{\kappa_2 + ix_2 - i\omega} - 1, \\ F_2(\omega) &= \frac{\sqrt{2\kappa_1 2\kappa_2} G_1 G_2}{D(\omega)(\kappa_1 - ix_1 + i\omega)(\kappa_2 + ix_2 - i\omega)}, \\ V_1(\omega) &= -\frac{iG_1\sqrt{2\kappa_1}}{D^*(-\omega)(\kappa_1 + ix_1 + i\omega)}, \\ V_2(\omega) &= -\frac{iG_2\sqrt{2\kappa_2}}{D(\omega)(\kappa_2 + ix_2 - i\omega)}, \\ D(\omega) &= -\frac{|G_1|^2}{\kappa_1 - ix_1 + i\omega} + \frac{|G_2|^2}{\kappa_2 + ix_2 - i\omega} + \left(\frac{\gamma_m}{2} - i\omega\right).\end{aligned}\quad (13)$$

The observed fields  $\delta a_{i\text{out}}(t)$  are related to  $\tilde{b}_{i\text{out}}(t)$  via

$$\delta a_{1\text{out}} = \delta b_{1\text{out}}e^{-i\omega_1 t} = \tilde{b}_{1\text{out}}e^{-i(\omega_1 - \omega_m)t} = \tilde{b}_{1\text{out}}e^{-i\omega_c t},\quad (14)$$

$$\delta a_{2\text{out}} = \delta b_{2\text{out}}e^{-i\omega_1 t} = \tilde{b}_{2\text{out}}e^{-i(\omega_1 + \omega_m)t} = \tilde{b}_{2\text{out}}e^{-i\omega_c t}.\quad (15)$$

Hence, we see that they have the simple relation  $\delta a_{i\text{out}} = \tilde{b}_{i\text{out}}e^{-i\omega_c t}$ . The above equations are valid under the condition that the system is in the stable regime. The sufficient and necessary condition for stability is that the coefficient matrix of the differential equations (9) by dropping fluctuating forces must have eigenvalues  $\lambda$  with negative real part,

$$\begin{vmatrix} -\gamma_m/2 - \lambda & iG_1 & -iG_2^* \\ -iG_1^* & -(\kappa_1 - ix_1) - \lambda & 0 \\ -iG_2 & 0 & -(\kappa_2 + ix_2) - \lambda \end{vmatrix} = 0.\quad (16)$$

By using the Routh-Hurwitz criterion [39], we get the stability condition  $|G_1|^2/\kappa_1 - |G_2|^2/\kappa_2 < \gamma_m/2$  when  $x_1 \sim x_2 \sim 0$ . If this condition is violated, the system goes into the instable regime.

We now give the meaning of the coefficients  $E_i$ ,  $F_i$  and  $V_i$  in (11) and (12). These coefficients are obtained to all orders in the strengths of the blue and red pumps. The  $E_i$ 's and  $F_i$ 's to second order in  $G_i$  can be given simple physical interpretations. Let us first consider an incoming vacuum photon from cavity 1. It should be borne in mind that the frequency  $\omega$  from the cavities corresponds to  $\omega_c + \omega$  according to Eqs. (14) and (15). This produces a vacuum photon of frequency  $\omega_c + \omega$  in cavity 1 and a photon of frequency  $\omega_c - \omega$  in cavity 2. The reason for the production of a photon of frequency  $\omega_c - \omega$  can be understood as follows: A blue detuned photon of frequency  $\omega_c + \omega_m$  produces a phonon of frequency  $\omega_m - \omega$  and a photon of frequency  $\omega_c + \omega$ . The phonon of frequency  $\omega_m - \omega$  interacts with the red detuned pump of frequency  $\omega_c - \omega_m$ . This is shown in the diagram in Fig 2. The term  $F_2(-\omega)$  in Eq. (12) represents the combined ef-

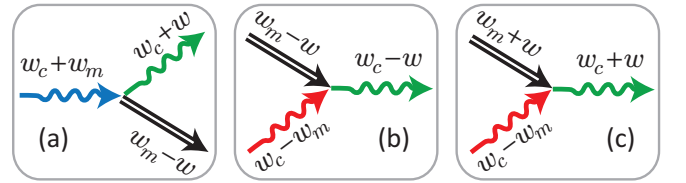


FIG. 2: The photon-phonon interaction processes in cavity 1 (a) and (c) and in cavity 2 (b).

fect of these two processes. We can similarly understand  $F_1(-\omega)$  in Eq. (11) by considering an incoming vacuum photon from cavity 2. Note that these are the diagrams which contribute to the lowest order in  $G_1 G_2$  in the expression for  $F_2(-\omega)$ . The term proportional to  $|G_1|^2$  in  $E_1(\omega)$  arises from the diagram Fig. 2(a). The  $V_i$  terms in (11) and (12) correspond to the quantum noise which is

added by either the thermal phonons or vacuum phonons. Note that in lowest order in  $G_i$ 's, we can interpret the last term in (12) by saying that a thermal phonon of frequency  $\omega_m + \omega$  combined with a red photon of frequency  $\omega_c - \omega_m$  to produce a photon of frequency  $\omega_c + \omega$  as shown in the Fig. 2(c). Similarly in Eq. (12) a thermal phonon or a vacuum phonon of frequency  $\omega_m - \omega$  and a photon of frequency  $\omega_c + \omega$  combine to create a blue photon  $\omega_c + \omega_m$ . This is the reverse of the process shown in Fig. 2(a).

### III. SQUEEZING SPECTRA

For studying squeezing spectra, we combine the output fields  $\delta a_{1\text{out}}$  and  $\delta a_{2\text{out}}$  to construct the field  $d$  as shown in Fig. 3. To make it more general, we add a phase

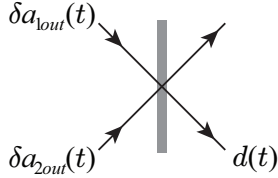


FIG. 3: The combination of the output fields  $\delta a_{i\text{out}}$ 's from two cavities using a 50/50 beam splitter.

difference  $\theta$  between the output fields, then  $d(t)$  can be written as

$$\begin{aligned} d(t) &= \frac{1}{\sqrt{2}}[\delta a_{1\text{out}}(t) + e^{i\theta}\delta a_{2\text{out}}(t)] \\ &= \frac{1}{\sqrt{2}}[\tilde{b}_{1\text{out}}(t) + e^{i\theta}\tilde{b}_{2\text{out}}(t)]e^{-i\omega_c t}. \end{aligned} \quad (17)$$

In the frame rotating with the cavity frequency  $\omega_c$ ,

$$\tilde{d}(t) = d(t)e^{i\omega_c t} = \frac{1}{\sqrt{2}}[\tilde{b}_{1\text{out}}(t) + e^{i\theta}\tilde{b}_{2\text{out}}(t)], \quad (18)$$

which obeys the commutation relation  $[\tilde{d}(t), \tilde{d}^\dagger(t')] = \delta(t - t')$ . The spectrum of  $\tilde{d}(t)$  can be calculated using Eqs. (11)-(13). We define as usual the quadrature variable  $X_\phi(t) = [\tilde{d}(t)e^{-i\phi} + \tilde{d}^\dagger(t)e^{i\phi}]/\sqrt{2}$ , and hence in the frequency domain

$$\begin{aligned} X_\phi(\omega) &= \frac{1}{\sqrt{2}}[\tilde{d}(\omega)e^{-i\phi} + \tilde{d}^\dagger(-\omega)e^{i\phi}] \\ &= \frac{1}{2}\left[\left(\tilde{b}_{1\text{out}}(\omega) + e^{i\theta}\tilde{b}_{2\text{out}}(\omega)\right)e^{-i\phi} \right. \\ &\quad \left. + \left(\tilde{b}_{1\text{out}}^\dagger(-\omega) + e^{i\theta}\tilde{b}_{2\text{out}}^\dagger(-\omega)\right)e^{i\phi}\right] \\ &= \frac{1}{2}\left[E(\omega)\tilde{b}_{1\text{in}}(\omega) + E^*(-\omega)\tilde{b}_{1\text{in}}^\dagger(-\omega) \right. \\ &\quad \left. + F(\omega)\tilde{b}_{2\text{in}}(\omega) + F^*(-\omega)\tilde{b}_{2\text{in}}^\dagger(-\omega) \right. \\ &\quad \left. + V(\omega)f(\omega) + V^*(-\omega)f^\dagger(\omega)\right], \end{aligned} \quad (19)$$

where

$$\begin{aligned} E(\omega) &= E_1(\omega)e^{-i\phi} + F_2^*(-\omega)e^{i\phi-i\theta}, \\ F(\omega) &= E_2(\omega)e^{i\theta-i\phi} + F_1^*(-\omega)e^{i\phi}, \\ V(\omega) &= V_1(\omega)e^{-i\phi} + V_2^*(-\omega)e^{i\phi-i\theta}. \end{aligned} \quad (20)$$

The squeezing spectrum defined as  $\langle X_\phi(\omega)X_\phi(\omega') \rangle = 2\pi S_\phi(\omega)\delta(\omega + \omega')$  can then be obtained using the correlation relations (4) and (10)

$$\begin{aligned} S_\phi(\omega) &= \frac{1}{2\pi} \int \langle X_\phi(\omega)X_\phi(\omega') \rangle d\omega' \\ &= \frac{1}{4} \left[ |V(\omega)|^2 \gamma_m (\bar{n}_{\text{th}} + 1) + |V(-\omega)|^2 \gamma_m \bar{n}_{\text{th}} \right. \\ &\quad \left. + |E(\omega)|^2 + |F(\omega)|^2 \right]. \end{aligned} \quad (21)$$

We note that if  $\tilde{d}(t)$  were a vacuum field, then

$$S_\phi(\omega) = 1/2 \quad (22)$$

Hence we define the normalized squeezing parameter as  $2S_\phi(\omega)$ . The magnitude of squeezing in dB units is then  $-10 \log_{10}(2S_\phi)$ .

### IV. SQUEEZING IN THE OUTPUT FIELDS FROM A DOUBLE CAVITY OPTOMECHANICS

We have studied the physics of the squeezing process in optomechanics in analogy to the down conversion process, and we expect Eq. (21) to yield squeezing. It is convenient to introduce the cooperativity parameter  $C_i = 2|G_i|^2/(\kappa_i\gamma_m)$  for each cavity  $i$ . We illustrate the

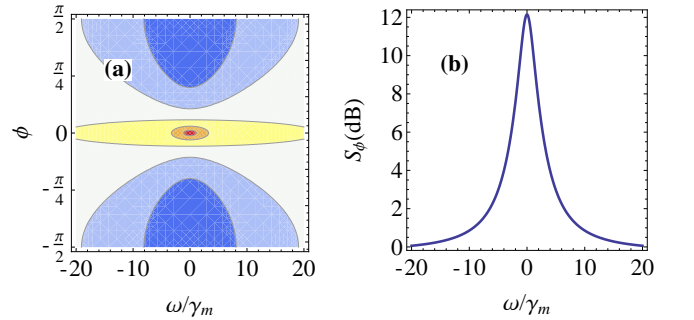


FIG. 4: (a) The density plot of the quadratures of the output field  $b(\omega)$  with  $-\Delta_1 = \Delta_2 = \omega_m$  at zero temperature. The middle region between the thick contours is squeezed. (b) The field amplitude ( $\phi = 0$ ) quadrature. The parameter set used in the plots are  $\omega_m = 2\pi \times 50\text{MHz}$ ,  $\kappa = 2\pi \times 1\text{MHz}$ ,  $\gamma_m = 2\pi \times 1\text{kHz}$ ,  $G_2 = i2\pi \times 0.1\text{MHz}$  ( $C_2 = 20$ ),  $G_1 = -G_2/\sqrt{2}$  ( $C_1 = 10$ ),  $x_1 = x_2 = 0$  and  $\theta = \pi$ .

features of our expected variance in the quadratures of the output field  $d(t)$  in Fig. 4(a) with  $\theta = \pi$  and for cooperativities  $C_2 = 2C_1 = 20$ . In the plot, we set  $\kappa_1 = \kappa_2 = \kappa$ . The complete set of parameters are given

in the caption. To create this map, we used Eq. (21) at zero temperature. In the diagram, we observe the largest magnitude of squeezing in the amplitude quadrature  $S_0$  (see Fig. 4(b)). The magnitude of squeezing at  $\omega = 0$  is about 12dB. As one rotates towards the phase quadrature  $S_{\pi/2}$ , the squeezing magnitude decreases and it eventually turns into antisqueezing.

It turns out that one can find the value of  $S_\varphi$  at  $\omega = 0$  analytically if we use the approximation  $\gamma, \kappa_i \ll \omega_m$  and  $C_{1,2} \gg 1$ , then

$$S_0(0) = \left| \frac{1 + \sqrt{C_1/C_2} e^{2i\phi - i\theta}}{1 - C_1/C_2} \right|^2 \left( \frac{1}{2} + \frac{2\bar{n}_{\text{th}} + 1}{2C_2} \right). \quad (23)$$

From which we find that  $S_0(0)$  approaches to its minimum value  $S_{\text{min}} = \frac{1 + (2\bar{n}_{\text{th}} + 1)/C_2}{2(1 + \sqrt{C_1/C_2})^2}$  if  $C_1/C_2 \rightarrow 1$  and  $\theta = \pi$ . Thus the squeezing reaches its maximum magnitude. Nonetheless, one also has to keep in mind of the stability condition from Eq. (16). Routh-Hurwitz stability criterion imposes the condition for the enhanced coupling rates into a dynamically stable range  $C_1 - C_2 < 1$ . In the resolved side-band limit and large cooperativity limit, it requires  $C_1 < C_2$ . Therefore, we can draw the conclusion that the effect of squeezing is optimized as  $C_1/C_2$  approaches from a small value to 1, which is the limit when instability occurs. This result is analogous, for example, to the result in optical bistability that squeezing increases as one approaches instability point.

We illustrate the dependence of the squeezing magnitude on the cooperativity parameter or on the pump power in Fig. 5. Fig. 5(a) shows the squeezing spectrum

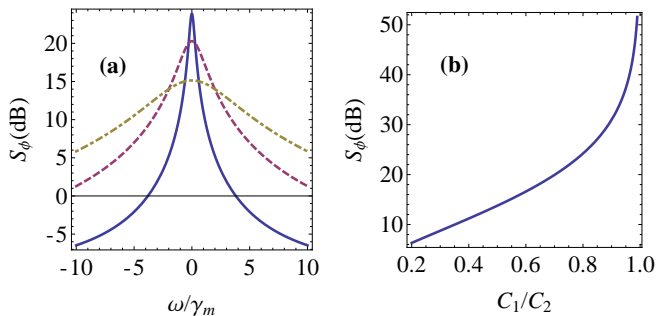


FIG. 5: (a) The field amplitude ( $\phi = 0$ ) quadrature with  $C_1/C_2 = 0.9$ (blue solid),  $= 0.7$ (red dashed) and  $= 0.5$ (yellow dotted) at zero temperature. (b) The squeezing spectrum at  $\omega = 0$  as a function of  $C_1/C_2$ . Other parameters used are  $\omega_m = 2\pi \times 50\text{MHz}$ ,  $\kappa = 2\pi \times 0.1\text{MHz}$ ,  $\gamma_m = 2\pi \times 1\text{kHz}$ ,  $G_2 = i2\pi \times 0.1\text{MHz}$  ( $C_2 = 20$ ),  $x_1 = x_2 = 0$  and  $\theta = \pi$ .

under different ratios of  $C_1/C_2$  and we see that squeezing spectrum gains magnitude but loses width when  $C_1/C_2$  increases from 0.5(dotted) to 0.7(dashed) and 0.9(solid). In Fig. 5(b), we plot Eq. (23) as a function of  $C_1/C_2$ , which shows that the magnitude of squeezing increases monotonically as  $C_1/C_2$  increases and it boosts very rapidly when  $C_1/C_2$  is close to 1. It should be borne

in mind that for  $C_1/C_2 \rightarrow 1$ , the system approaches to the threshold for instability. When it is too close to the threshold, the linearization procedure used to calculate fluctuations begins to break down.

The physics in the generation of the squeezed vacuum states can be interpreted using the FWM process via phonons, as shown in Fig. 6. In cavity 1, A blue detuned

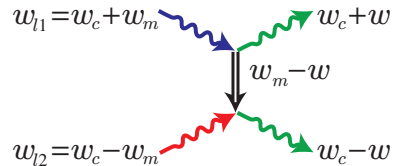


FIG. 6: Generation of squeezed states via phonons in FWM process.

driving laser photon ( $\omega_{l1} = \omega_c + \omega_m$ ), when being scattered by the mechanical oscillator, produces a phonon ( $\omega_m - \omega$ ) and a photon at a lower frequency  $\omega_c + \omega$ . At the same time in cavity 2, a red detuned driving laser photon ( $\omega_{l2} = \omega_c - \omega_m$ ) by absorbing a phonon ( $\omega_m - \omega$ ) and produces a photon at  $\omega_c - \omega$ . These processes are resonantly enhanced if both the generated photons are close to the cavity resonance frequency. Equivalently, the physics can be described by the effective Hamiltonian for the FWM process in Fig. 6:  $a_{l1}a_{l2} \int \Phi(\omega) a_{\omega_c - \omega}^\dagger a_{\omega_c + \omega}^\dagger d\omega + h.c. \approx$

$\alpha \int \Phi(\omega) a_{\omega_c - \omega}^\dagger a_{\omega_c + \omega}^\dagger d\omega + h.c.$ , when the strong driving lasers can be approximated classically by a number  $\alpha$ . Here  $\Phi(\omega)$  depends on the details of the optomechanical cavities. Such an interaction has been extensively studied in quantum optics [18–20] and is known to lead to the generation of quantum entanglement as well as quantum squeezing. In the context of the double cavity optomechanics, the generation of entangled pairs has been discussed previously [4].

## V. EFFECT OF THE BROWNIAN NOISE OF THE MIRROR ON SQUEEZING

It is known that the squeezing is degraded by any kind of noise effects. In optomechanics, the Brownian noise of the mirror makes the observation of quantum effects difficult. We now investigate the effect of the  $V$  terms in Eq. (19) on the possible amounts of squeezing. In Fig. 7, we plot the output field amplitude quadrature at finite temperatures. Comparing the solid curves in (a) and (b), they have a common cooperativity parameter  $C_2 = 20$  but different bath temperatures. In (a), at  $T = 3.5\text{mK}$  correspondingly  $\bar{n}_{\text{th}} = 1$ , strong squeezing with magnitude as high as 11dB can be observed; while in (b), at  $T = 10\text{mK}$  correspondingly  $\bar{n}_{\text{th}} = 3.7$ , the squeezing magnitude drops to 8 dB. Interestingly, in our system, the decreasing of squeezing due to rising bath temperature can be compensated by increasing

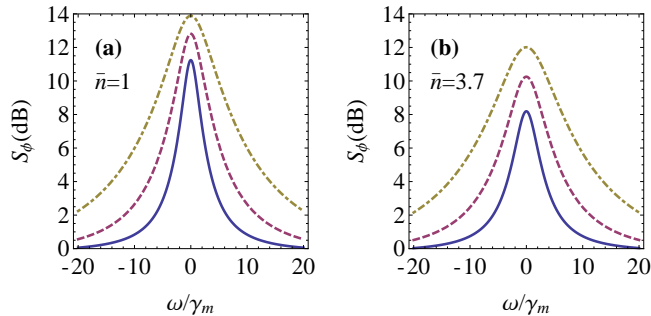


FIG. 7: The spectrum of amplitude quadrature ( $\phi = 0$ ) with fixed  $C_2/C_1 = 1/2$  and  $C_2 = 20$  (blue solid),  $= 40$  (red dashed) and  $= 80$  (yellow dotted). The bath temperatures are (a)  $T = 3.5\text{mK}$  correspondingly  $\bar{n}_{\text{th}} = 1$ ; and (b)  $T = 10\text{mK}$  correspondingly  $\bar{n}_{\text{th}} = 3.7$ . Other parameters are the same as in Fig. 4.

the cooperativity, in way of enhancing the coupling constant or reducing decaying rates. Now we concentrate on Fig. 7(b), in which  $\bar{n}_{\text{th}} = 3.7$  and squeezing magnitude is 8dB. When we increase  $C_2$  from 20 (solid) to 40 (dashed) and to 80 (dotted), we can clearly see the squeezing magnitude increased to 10dB and 12dB. The width of the

squeezed spectrum is increased as well. This agrees with Eq. (23) from which we find increasing  $C_2$  essentially reduces the effect of  $\bar{n}$ . The equation (23) also suggests that a larger cooperativity is always preferable in order to generate large squeezing magnitude at nonzero temperature, although it never exceeds the zero temperature case. One has squeezing as long as the right hand side of Eq.(23) is less than 0.5. For  $C_2 = 2C_1 = 20$ ,  $S_0(\omega)$  has the value  $0.189 + 0.034\bar{n}_{\text{th}}$ .

## VI. CONCLUSIONS

In conclusion, we have shown how squeezing of the order of 10dB can be generated in a double cavity optomechanical system. We searched for conditions under which the double cavity optomechanical system would lead to the generation of the photon pairs. We show that such a photon pair generation can be described by an effective interaction which are used for generating squeezing using parametric down conversion and four-wave mixing. However, there is one significant difference. We generate photon pairs by using active participation of phonons. The phonon mediated processes lead to additional noise terms which degrade squeezing.

- 
- [1] A. Nunnenkamp, K. Børkje, and S. M. Girvin, Phys. Rev. Lett. **107**, 063602 (2011).
- [2] A. Kronwald and F. Marquardt, Phys. Rev. Lett. **111**, 133601 (2013).
- [3] A. Heidmann, Y. Hadjar, M. Pinard, Appl. Phys. B **64**, 173(1997).
- [4] Y. -D. Wang and A. A. Clerk, Phys. Rev. Lett. **110**, 253601 (2013); L. Tian, Phys. Rev. Lett. **110**, 233602 (2013).
- [5] Y. -D. Wang and A. A. Clerk, Phys. Rev. Lett. **108**, 153603 (2012); L. Tian, Phys. Rev. Lett. **108**, 153604 (2012).
- [6] J. Li, S. Gröblacher, and M. Paternostro, New J. Phys. **15**, 033023 (2013).
- [7] S. Huang and G. S. Agarwal, Phys. Rev. A **82**, 033811 (2010); T. Weiss, C. Bruder, A. Nunnenkamp, New J. Phys. **15**, 045017 (2013).
- [8] T. Botter, D. W. C. Brooks, N. Brahm, S. Schreppler, Dan M. Stamper-Kurn, Phys. Rev. A **85**, 013812 (2012).
- [9] Y. -C. Liu, Y. -F. Xiao, Y. -L. Chen, X. -C. Yu, and Q. Gong, Phys. Rev. Lett. **111**, 083601 (2013).
- [10] M. -A. Lemonde, N. Didier, and A. A. Clerk, Phys. Rev. Lett. **111**, 053602 (2013).
- [11] K. Børkje, A. Nunnenkamp, J. D. Teufel, and S. M. Girvin, Phys. Rev. Lett. **111**, 053603 (2013).
- [12] S. P. Tarabrin, H. Kaufer, F. Ya. Khalili, R. Schnabel, K. Hammerer, Phys. Rev. A **88**, 023809 (2013).
- [13] G. -F. Xu and C. K. Law, Phys. Rev. A **87**, 053849 (2013).
- [14] M. Asjad, J. Russ Laser Res. **34**, 159 (2013).
- [15] T. A. Palomaki, J. W. Harlow, J. D. Teufel, R. W. Simmonds, and K. W. Lehnert, Nature **495**, 210 (2013).
- [16] G. Kirchmair, B. Vlastakis, Z. Leghtas, S. E. Nigg, H. Paik, E. Ginossar, M. Mirrahimi, L. Frunzio, S. M. Girvin, and R. J. Schoelkopf, Nature **495**, 205 (2013).
- [17] W. Ge, M. Al-Amri, H. Nha, M. S. Zubairy, Phys. Rev. A **88**, 052301 (2013).
- [18] L. Mandel, E. Wolf, Optical Coherence and Quantum Optics (Cambridge University Press, 1995), Chap. 21.
- [19] D. F. Walls and G. J. Milburn, Quantum Optics (Springer-Verlag, Berlin, 1998), Chap. 8.
- [20] G. S. Agarwal, Quantum Optics, (Cambridge University Press, 2012), Chap. 3.
- [21] D. J. Wineland, J. J. Bollinger, W. M. Itano, and D. J. Heinzen, Phys. Rev. A **50**, 67 (1994).
- [22] R. McConnell, H. Zhang, S. Čuk, J. Hu, M. H. Schleier-Smith, and V. Vuletić, Phys. Rev. A **88**, 063802 (2013).
- [23] G. A. Garrett, A. G. Rojo, A. K. Sood, J. F. Whitaker and R. Merlin, Science, **275**, 1638(1997).
- [24] L. Duan, M. Lukin, J. I. Cirac, and P. Zoller, Nature **414**, 413, (2001).
- [25] F. Brennecke, S. Ritter, T. Donner, T. Esslinger, Science, **322**, 235(2008).
- [26] J. Lian, L. Yu, J.-Q. Liang, G. Chen, and S. Jia, Scientific Reports **3**, 3166 (2013).
- [27] B. Lücke, M. Scherer, J. Kruse, L. Pezzé, F. Deuretzbacher, P. Hyllus, O. Topic, J. Peise, W. Ertmer, J. Aert, L. Santos, A. Smerzi, and C. Klempt, Science **334**, 773, (2011).
- [28] C. M. Caves, K. S. Thorne, R. W. P. Drever, V. D. Sandberg, and M. Zimmermann, Rev. Mod. Phys. **52**, 341 (1980).
- [29] V. B. Braginsky, Y. I. Vorontsov, K. S. Thorne, Science

- 209**, 547 (1980).
- [30] B. Yurke, S. L. McCall, and J. R. Klauder, *Phys. Rev. A* **33**, 4033 (1986).
- [31] A. A. Clerk, F. Marquardt, and K. Jacobs, *New J. Phys.* **10**, 095010 (2008).
- [32] K. Jähne, C. Genes, K. Hammerer, M. Wallquist, E. S. Polzik, and P. Zoller, *Phys. Rev. A* **79**, 063819 (2009).
- [33] M. Tsang and C. M. Caves, *Phys. Rev. Lett.* **105**, 123601 (2010).
- [34] D. W. C. Brooks, T. Botter, S. Schreppler, T. P. Purdy, N. Brahms, and D. M. Stamper-Kurn, *Nature* **488**, 476 (2012).
- [35] A. H. Safavi-Naeini, S. Gröblacher, J. T. Hill, J. Chan, M. Aspelmeyer, and O. Painter, *Nature (London)* **500**, 185 (2013).
- [36] T. P. Purdy, P.-L. Yu, R. W. Peterson, N. S. Kampel, and C. A. Regal, *Phys. Rev. X* **3**, 031012 (2013).
- [37] M. Asjad, G. S. Agarwal, M. S. Kim, P. Tombesi, G. Di Giuseppe, D. Vitali, arXiv:1309.5485.
- [38] M. Karuza, C. Biancofiore, M. Bawaj, C. Molinelli, M. Galassi, R. Natali, P. Tombesi, G. Di Giuseppe, and D. Vitali, *Phys. Rev. A* **88**, 013804 (2013); M. Karuza, C. Molinelli, M. Galassi, C. Biancofiore, R. Natali, P. Tombesi, G. Di Giuseppe, and D. Vitali, *New J. Phys.* **14**, 095015 (2012).
- [39] A. Hurwitz, On the conditions under which an equation has only roots with negative real parts. *Selected Papers on Mathematical Trends in Control Theory.* (Dover, New York, 1964).